Phele, M., & Mtunzi, F. (2024.). Sequestration of ciprofloxacin from aqueous solutions by nanocomposite obtained via *Moringa Oleifera* pods and feldspar clay modification. *STED Journal*, *6*(2), 25-38.

SEQUESTRATION OF CIPROFLOXACIN FROM AQUEOUS SOLUTIONS BY NANOCOMPOSITE OBTAINED VIA *MORINGA OLEIFERA* PODS AND FELDSPAR CLAY MODIFICATION

Mokete Phele[1,2], Fanyana Mtunzi[1,2]

[1]Department of Biotechnology and Chemistry, Faculty of Applied and Computer Sciences, Vaal University of Technology, Vanderbijlpark, 1911, South Africa, phelemj85@gmail.com
[2]Institute of Chemical and Biotechnology, Faculty of Applied and Computer Sciences, Vaal University of Technology Southern Gauteng Science and Technology Park, Sebokeng, 1983, South Africa

ORIGINAL SCIENTIFIC PAPER

ISSN 2637-2150
e-ISSN 2637-2614
UDC 633.853.492:582.683.4
DOI 10.7251/STEDZ2402025P
COBISS.RS-ID 141779457

Received: 24 July 2024.
Accepted: 17 November 2024.
Published: 29 November 2024.
http://stedj-univerzitetpim.com

Corresponding Author:
Mokete Phele, Department of Biotechnology and Chemistry, Faculty of Applied and Computer Sciences, Vaal University of Technology, Vanderbijlpark, 1911, South Africa, phelemj85@gmail.com

Citation:
Phele, M., & Mtunzi, F. (2024.). Sequestration of ciprofloxacin from aqueous solutions by nanocomposite obtained via *Moringa Oleifera* pods and feldspar clay modification. *STED Journal*, *6*(2), 25-38.

ABSTRACT

The environmental hazards of antibiotics have captivated increasing research focus, but their environmental behaviours remain unclear in water sources. Thus, this study focused on exploring the interaction mechanisms between *Moringa Oleifera* pod-modified feldspar clay (MFC) and ciprofloxacin (CIP) during sorption process. The efficiency of these adsorbents in aqueous solution adsorption of CIP were investigated as a function of pH, time and sorbate concentration. The impact of pH solution and CIP evolution showed that CIP sorption on MFC is strongly reliant on pH solution. Kinetic studies authenticated that the CIP sorption mechanism was a physisorption involving ion exchange and surface complexation mechanisms. The mechanism of CIP sorption on MFC was successfully studied using characterization techniques. The Langmuir and Freundlich isotherm equations were used to analyze the equilibrium isotherm data. The adsorption process fitted well with the second-order kinetics and the Langmuir isotherm equation fitted well with the experimental data. The Langmuir isotherm showed that maximum adsorption capacity was found to be 57.61 mg. g^{-1}. Thermodynamic factors: ΔG° values of -29 $kJ.mol^{-1}$, ΔH° = 17 $kJ.mol^{-1}$, and ΔS° = 163 $J.mol^{-1}$ k of CIP adsorbed onto MFC indicate that the adsorption was spontaneous and endothermic in nature.

Keywords: *Moringa Oleifera*, Carbonaceous materials, feldspar clay, Ciprofloxacin, Sorption

INTRODUCTION

Due to the potential harm to the environment and the effects on the health of people and animals, there is a great deal of concern about the removal of pollutants from aquatic ecosystems. Anything that is present in the aquatic environment at a negligible concentration and whose presence is not entirely certain is considered an emerging contaminant (EC) (Rodriguez-Narvaez, Peralta-Hernandez, Goonetilleke, & Bandala, 2017). Antibiotics are commonly used to treat bacterial illnesses in human therapy and as veterinary drugs to forestall illnesses in livestock, and also feature as increase promoters, normally in farm animals (Kümmerer, 2009). With the high rate of different antibiotics in use, extensive amount of pharmaceutical wastewater containing antibiotics has been acquitted into the surroundings (Hartmann, Golet, Gartiser, Alder, & Koller, 1999), they are also not definitely digested in the human/animal body, but emanated by way of urine, animal dung and/or faeces. Ciprofloxacin (CIP), one of the most generally used antibiotics in the therapy of infectious diseases (Martins, Vasconcelos, Henriques, Frank, König, & Kümmerer, 2008; Hartmann, Alder, Koller, & Widmer, 1998; Hartmann, 1998), is not comfortably biodegradable (Hirsch, Ternes, Haberer, & Kratz, 1999) and has extreme toxic aspect consequences such as stomatitis, leukopenia and emesis in humans (Kümmerer, Al-Ahmad, & Mersch-Sundermann, 2000; Cox, et al., 2002). Excessive occurrence of CIP in the marine environment can also yield an increase in antibiotic-resistant bacteria (Diwan, et al., 2010) and adverse effects on water quality (Chang, et al., 2010).

However, less studies have dealing at the eradication of CIP from water correlate to other antibiotics. Considerable strategies have been utilized for CIP elimination, including chemical oxidation and electrochemistry (Xiao, Zeng, & Lemley, 2010), oxidation by chlorination (Li, & Zhang, 2012), ozonation (Nasuhoglu, Rodayan, Berk, & Yargeau, 2012), photolytic and photocatalytic treatment (Vasquez, Hapeshi, Fatta-Kassinos, & Kümmerer, 2013), Photo-Fenton oxidation processes (Sun, et al., 2009), and enzymatic degradation and biological treatment (Dorival-García, Zafra-Gómez, Navalón, González, & Vílchez, 2013), and adsorption (Chen, Gao, & Li, 2015; Maged, Kharbish, Ismael, & Bhatnagar, 2020). To a certain extent these techniques are notorious for their high cost of implementation or poor ability to achieve respectable water quality, with the exception of adsorption. Thus, biological materials, nanomaterials and clays have all been explored as low-cost adsorbents for the elimination of antibiotics from aqueous solutions and wastewaters.

Studies have exemplified different methods of Ciprofloxacin (CIP) removal from the water systems. Acid-activated bentonite clay mineral has been used to evaluate the interaction of nanocomposites with ciprofloxacin (CIP) during sorption process from aqueous solution (Maged, et al., 2020). In this time consuming work the maximal monolayer sorption capacity of 305.20 mg. g^{-1} was observed, while effect of CIP speciation and the pH value of solution demonstrate that CIP sorption onto bentonite is greatly dependent on pH value, and sorption mechanism as chemisorption as revealed by the kinetic studies. Fluoroquinolone antibiotic levofloxacin (LEVO) in water was removed by ozonation and photo catalysis (UVC lamp (254 nm), TiO_2) (Nasuhoglu, et al., 2012). It was observed that after an ozone dose of 20.5 mg/L and 180 min of photocatalytic oxidation, LEVO at initial concentration (Co = 20 mg/L) was no longer detected.

Ciprofloxacin hydrochloride was effectively degraded by Photo-Fenton oxidation process under optimum conditions of $C_0 = 15$ mg/L, pH 4.0, $[Fe^{2+}] = 0.05$ mmol/ L, $[H_2O_2] = 5.0$ mmol/L, and 25°C, it was observed that in the 45-min reaction time, no ciprofloxacin hydrochloride was detected. It was determined that the degradation kinetics of ciprofloxacin hydrochloride by this process followed the first-order reaction kinetics model (Sun, et al., 2009). The capability and mechanism of graphene-oxide to remove ciprofloxacin (CIP) and sulfamethoxazole (SMX) from aqueous solution was reported to effectively adsorb both sulfamethoxazole and ciprofloxacin with maximum sorption capacity of 240 and 379 mg/g, respectively (Chen, Gao, & Li, 2015). Commonly found quinolones (ciprofloxacin, norfloxacin, pipemidic acid, moxifloxacin, piromidic acid, and ofloxacin), in wastewaters from a wastewater treatment plant, were removed by sorption and biological degradation in laboratory-scale membrane bioreactors (MBR) pilot plant (Dorival-García, et al., 2013). Sorption on the sludge played a prevailing role in the elimination of the antibiotics from waters as indicated by mass balances. In this investigation it was estimated that the sorption coefficient K_d values were between 516 and 3746 L/kg within temperature range of 9–38 °C.

The study focuses on a composite of *Moringa oleifera* pod and feldspar clay, which is one of many natural adsorbents. Synergistic combinations of feldspar clay (FLC) and *Moringa oleifera* pod (MOP) (both low-cost adsorbents) were achieved in this study by associating individual properties of each composite to yield a superior adsorbent with properties such as high cation exchange capacity, bleeding elimination, increased mechanical strength and higher adsorption efficiency for water treatment. After full characterization of the adsorbent, the effect of solution pH, adsorbent dose and contact time on the adsorption capacity was investigated. The adsorption kinetics and thermodynamics were also studied.

EXPERIMENTAL

Materials

All used chemicals were of analytical grade. Ciprofloxacin hydrochloride (CIP) with a purity higher than 99.6% was purchased from Sigma-Aldrich. Ultrapure water purified in a Milli-Q system (pH 7 ± 0.2) was used for this study.

Preparation of Feldspar Clay

Feldspar clay (FLC) was obtained from the clay reserve of Federal Institute of Industrial Research Oshodi (FIIRO), Lagos, Nigeria. The clay was pre-treated by suspending in deionized water in order to remove sand and heavy non-clay materials. Organic matter in the clay was then removed by treatment with 30% hydrogen peroxide (H_2O_2) solution (Diagboya, Olu-Owolabi, & Adebowale, 2015). This was followed by washing with distilled water, drying at 105°C, sieving using a mesh size sieve, and stored.

Collection and Preparation of *Moringa Oleifera* Pods

Moringa oleifera pods (MOP) were collected from trees in Limpopo farm near Polokwane. Soon after collection, pods were washed thoroughly with doubly distilled deionized water to remove water soluble impurities and oven dried at 105°C for 24 h. The washed and dried material was pulverized (by mortar and pestle) and sieved to different mesh sizes. The sieved material was rewashed thoroughly with doubly distilled deionized water to remove the fine particles and dried at 105°C for 4 h. The material was treated with 0.1M nitric acid and methanol for 4 h to remove inorganic and organic matter from the sorbent surface and dried in an electric furnace. The treated and untreated materials were placed in a desiccator to be used as sorbents.

Preparation of *Moringa Oleifera pod* and Feldspar Clay Composite

Equal weight of FLC and MOP (5.0 g each) were weighed into a 250 m beaker, containing 300 mL of 0.1 M NaOH solution. The content was thoroughly stirred and heated in an oven at 105℃ until dryness. The dried samples mixture was weighed into crucibles and calcined at 300℃ in a furnace for 6hrs. The resulting dark powdery material was washed with deionized water to remove all carbon materials on the surface of the composite and was subsequently dried to remove all moisture (Unuabonah, Gunter, Weber, Lubahn, & Taubart, 2013). The dried sample was stored in an airtight container and referred as MFC.

ADSORPTION EXPERIMENTS

Adsorption of ciprofloxacin

Experiments were performed with 250 mL glass Erlenmeyer flasks. Each flask contained 50 mL of CIP solution. A certain amount of adsorbent was mixed with the solution, and the resulting mixture was shaken at 130 rpm and 15 °C in a shaker. The solution pH was adjusted with 0.1 mol/L HCl and 0.1 mol/L NaOH solutions. The CIP concentrations were measured by Ultraviolet–visible spectroscopy spectrophotometry at 271 nm. The adsorption capacity (q_e, mg/g) was calculated through Eq. (1):

$$q_e = \frac{(C_0 - C_e)}{M} V \qquad (1)$$

where C_o and C_e are the initial and final pollutant concentrations (mg/L), respectively, while M (mg) and *V* (mL) are the MFC mass and solution volume, respectively. The vials were kept in the dark and were shaken in a rotary shaker at 15 °C for 72 h which was sufficient to reach apparent equilibrium.

Adsorption Isotherm of MFC

The initial CIP concentration was varied from 10 to 60 mg/L. Langmuir and Freundlich for the adsorption isotherm were used to analyse the experimental data.

Adsorption kinetics determination

For the studies on the adsorption kinetics, 0.02 g adsorbent was added to 50 ml of a 10 mg/L CIP solution. The contact time ranged from 0 to 160 min. The flasks were shaken at 130 rpm at a temperature of 15 °C. Pseudo-first order (Eq. (2)) and pseudo-second order (Eq. (3)) models for the adsorption kinetics were used to analyze the experimental data.

$$log(q_e - q_t) = log q_e - \frac{k_1 t}{2.303} \qquad (2)$$

$$\frac{t}{q_t} = \frac{1}{k_1 {q_e}^2} + \frac{t}{q_e} \qquad (3)$$

Where q_e is the mass of CIP adsorbed at equilibrium (mg/g), qt is the mass of CIP adsorbed at time t (min), and k_1 and k_2 are the pseudo-first order model and the pseudo-second order model rate constants of adsorption.

Adsorption thermodynamics

In order to understand the adsorption process, the three main adsorption thermodynamic parameters, standard free energy (ΔG^0), standard enthalpy (ΔH^0), and standard entropy (ΔS^0), were calculated. The thermodynamic equilibrium constant is approximately equal to the Langmuir adsorption constant (Liu, 2009). The thermodynamic parameters were calculated through the following equations:

$$\Delta G = -RT\, InK_L \qquad (4)$$

where K_L is the equilibrium constant obtained from Langmuir model, T the absolute temperature (K) and the universal gas constant $R=8.314\times10^{-3}$ $kJK^{-1}mol^{-1}$. The relationship between K and thermodynamic parameters of ΔH and ΔS can be described by the Van't Hoff correlation in the following equation (Celik, & Ozdermir, 2018; Yildiz, Erol, Aktas, & Alimli, 2004):

$$InK = \frac{\Delta S}{R} - \frac{\Delta H}{RT} \qquad (5)$$

Sample preparation for FTIR analysis

An approximately amount of 150 mg of potassium bromide (KBr) was mixed with about 1 mg of the sample. The mixture was crushed using pestle and mortar, thereafter a small amount of the crushed fine powder was loaded into three pieces of the pellet press using spatula. The three pieces of the pellet press was transferred to hydraulic press for compression for about 2 minutes. The resulted pellets were introduced into FTIR instrument for analysis. The experimental condition for FTIR analysis are shown in Table 1.

Table 1 Experimental conditions for FTIR analysis.

Name of the instrument	**Bruker-Alpha, Germany**
Parameter	
Scan range	400-4500 cm^{-1}

Scanning Electron Microscope (SEM)

Scanning electron microscopy (SEM) was used to observe the microstructure and surface morphology of MOP, FLC and MFC. The SEM images were obtained on a Cerl-Zeiss Sigma instrument (Germany) that uses a tungsten filament source. The samples were Pd-Au coated, and imaging was done at 5 kV.

RESULTS AND DISCUSSION

The major functional groups present in the MOP and FLC were characterized by infrared analysis. In the Figure 1 are given FTIR spectra of *M.Oleifera* pods, FLC and MFC.

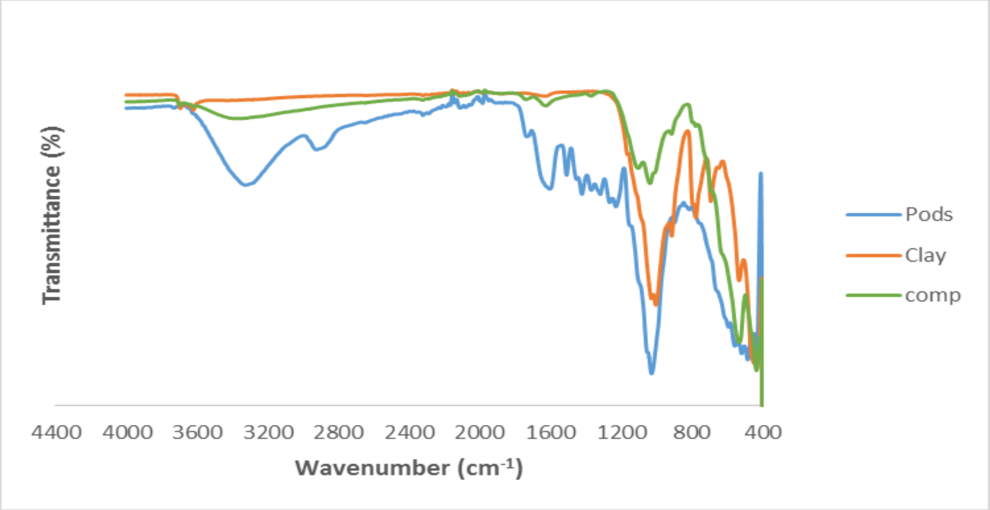

Fig. 1. FTIR spectra *M.Oleifera* pods, FLC and MFC

The broad spectrum centered at 3326 cm^{-1} can be attributed to O-H stretching of the linkage in this protein, fatty acids, carbohydrates and the lignin units. Due to the high protein content of seeds, there is also a relevant contribution to this region because of N-H stretching in amide binding (Stuart, 2004). The peaks appearing at 2970 and 2888 cm^{-1} correspond to asymmetric and symmetric stretching of the C-H to CH$_2$ group compound, respectively. In the 1800 to 1500 cm^{-1} region there is a series of overlapping bands between 1750 and 1630 cm^{-1}. This set can be attributed to the elongation of the C=O bond. Due to the heterogeneous pod type, the carbonyl group can be attached to different adjacencies as part of the fatty acid portion of the lipid and the protein portion of the amides. The carbonyl occurring at 1741 and 1713 cm^{-1} due to the lipid component, which can be observed in the spectrum as a small peak or shoulder part of the main band at 1656 cm^{-1}, was assigned to the carbonyl amides in the protein portion. The peak at 1585 cm^{-1} can be attributed to the stretching of the C-N linkage and the deformation of the N-H linking proteins present in the seed coat.

The IR spectra of feldspar show a broad amplitude vibration around 1002 cm^{-1}. Furthermore, show vibrations represented by peak between 427 cm^{-1} and 467.30 cm^{-1}, around 693 cm^{-1} and 795 cm^{-1}, around 912 cm^{-1}, 1007 cm^{-1}, 1122 cm^{-1}, 1634 cm^{-1}, 3443 cm^{-1}, 3624 cm^{-1}, 3654 cm^{-1} and 3694 cm^{-1}. As shown in Figure 1, the OH stretching region is between 3805 cm^{-1} and 3408 cm^{-1} (region with strong hydrophilic effect), and the FTIR spectral studies of feldspar show three bands in this region. The extensional vibration mode observed at 1122 cm^{-1}, 1034 cm^{-1}, 1007 cm^{-1} are certainly different vibrational modes of Si-O such as quartz stretching, longitudinal mode and typical extensional mode. The Al-OH-Al bending mode is found at 912 cm^{-1}.

Surface morphology

The SEM images of the MOP biomass were inherently foamy and fibrous with no specific shape as reported elsewhere (Tavengwa, Cukrowska, & Chimuka, 2016). However, after thermal treatment (250°C), the surface morphology showed macropores and irregular gully-like patterns. The structure appeared weak and the cell morphology of the biochar was absent. The micrographs of MOP

(Figure 2) show mesoporous structures with different pore sizes. These surface properties would result in high drug bonding due to the available bonding voids for CIP. Comparing the surface features of FLC and MOP under SEM provides clear differences. The feldspar emerges like a microcrystalline material while MOP appears like a cryptocrystalline material. This manner that between the two adsorbents FLC, MOP, the most crystalline morphology is in FLC although it looks like flakes or plates. MOP has a less crystalline (amorphous) morphology.

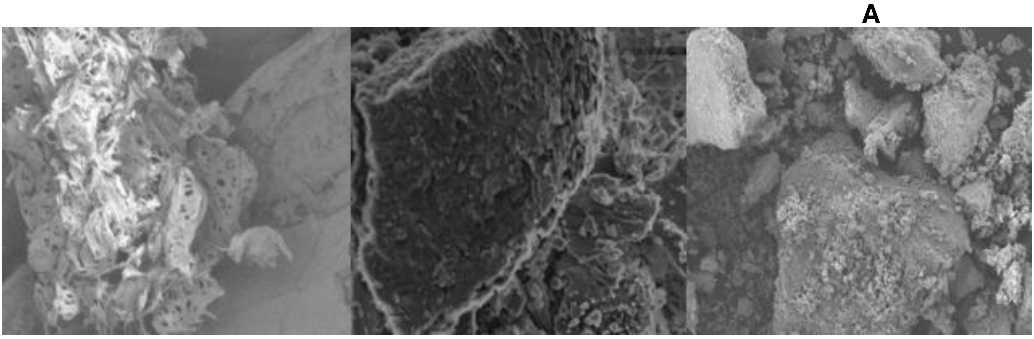

Fig. 2. Scanning electron microscopy images of (A) MOP, (B) FLC and (C) MFC

Effect of adsorbent dose on CIP adsorption

To enhance the quantity of MFC mass essential to achieve utmost CIP sorption, the impact of MFC dosage on CIP elimination efficiency and sorption capacity was evaluated. Sorbent CIP (%) versus adsorbent dosage is plotted in Figure 3. The results obtained showed that the percentage of CIP elimination deliberately elevated with the increase in *Moringa*-clay mass. The surface area and available binding sites increasing could be the cause of this behaviour. The influence of the adsorbent dose (0.1-0.6 g/L) at an initial CIP concentration of 10 mg/L was tested at 15 °C. As shown in Figure 3, the results show that the CIP removal rate increased sharply with increasing adsorbent dose (from 0.1 to 0.2 g/L) and then increased more slowly from 0.2 to 0.6 g/L.

This result may be due to the increase in the number of adsorption sites when the amount of adsorbent increased. This could be attributed to the moringa-clay composite which furnish more surface-active sites for sorption of CIP molecules. Therefore, 0.3 g/L of the adsorbent dose was used in subsequent experiments.

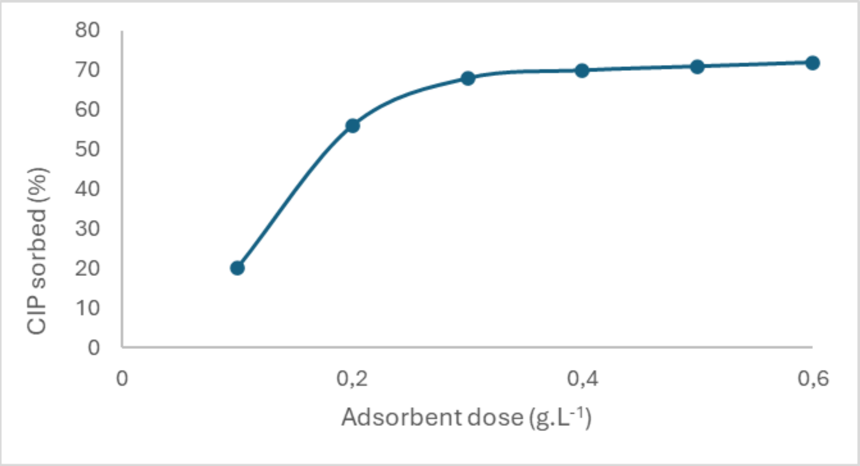

Fig. 3. Effect of adsorbent dose on the CIP sorbed.

Effect of contact time

The percentage of CIP removal increased with increasing contact time (Figure 4). The uptake of CIP was quick in the first 40 minutes and after 60 minutes the amount of CIP adsorbed remained almost constant. Therefore, 60 minutes was chosen as the equilibrium time in the present study. At the beginning of the reaction, adsorption was fast because many vacancies were available (Zhang, Qiao, Zhao, & Wang, 2011). In contrast, the slow adsorption might have been due to insufficient vacancies. The percent adsorption increased from 21.2 to 87.4 over a contact time of 10 to 60 minutes.

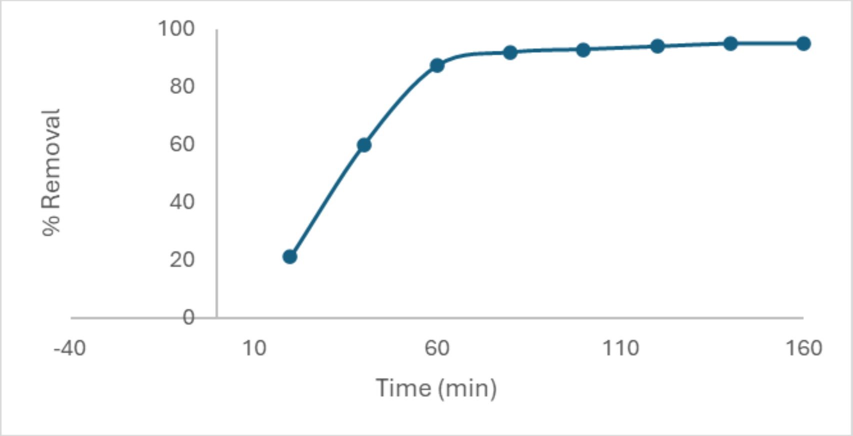

Fig. 4. Effect of contact time on CIP sorbed

Effect of pH

CIP sorption is greatly affected by solution pH due to the different CIP speciation as well as the surface charge of *Moringa*-clay adsorbents. In general, the adsorption of ionizable organic contaminants is influenced by pH due to the different species (Zhang, Pan, Zhang, Ning, & Xing, 2010). CIP has positively charged (cationic), negatively charged (anionic) and/or zwitterionic species at different pH values due to different pK_as (5.9 and 8.9) (Gu, & Karthikeyan, 2005). The cationic CIP form (CIP^+) is present when the pH of the solution is less than pK_{a1} (= 5.9), which is owing to the protonation of the amine group. In acidic and neutral aqueous solutions, a stoichiometric exchange between CIP and interlayer cations resulted in a high adsorption capacity. When the solution pH was above its pK_{a2} (8.7), the adsorption of CIP was significantly reduced due to the net repulsion between the negatively charged surfaces and the CIP anion (Li, Schulz, Ackley, & Fenske, 2010). The widespread use of *moringa* and feldspar clay composite can be associated to its physical and chemical properties such as small particle size, high porosity, large surface area and high cation exchange capacity.

When the pH of the solution is higher than pK_{a2} (= 8.7), the anionic CIP form (CIP^-) exists due to the deprotonation of the amine group. At a solution pH between pK_{a1} and pK_{a2}, the CIP molecule becomes a zwitterion ($CIP^{\pm}$) (Wang, Li, Jiang, Jean, & Liu, 2010). This conduct is owing to the protonation and deprotonation of the amine group and the carboxylic acid group (Jiang, et al., 2013). Figure 5 display the impact of pH solution on CIP sorption by MFC. It was observed that the CIP elimination elevated barely when the pH was less than pK_{a1}, confirming the CIP (cationic form) speciation. Thus, the sorption mechanism of CIP mainly involves cation exchange and interlayer complexation between MFC and CIP molecules. At a pH range of 5–6, CIP sorption was favored due to the electrostatic attraction between negative surface charge of MFC and positive charge on the CIP molecule. When the pH of the solution is ($pK_{a1} < pH < pK_{a2}$), the MFC surface becomes negatively charged and the CIP molecules are in zwitterionic form. Hence, positively charged amine groups in zwitterionic form could still donated to CIP sorption through the cation exchange mechanism, and CIP sorption was still high (Genc, Dogan, & Yurtsever, 2013). Subsequently, a sharp reduce in CIP sorption occurred when the pH of the solution became higher than pK_{a2}. This reduction could be explained by the repulsion between the anionic CIP form and the negatively charged *Moringa*-clay surface. The optimal pH has been determined to be 7 since the maximum CIP adsorption capacity occurs.

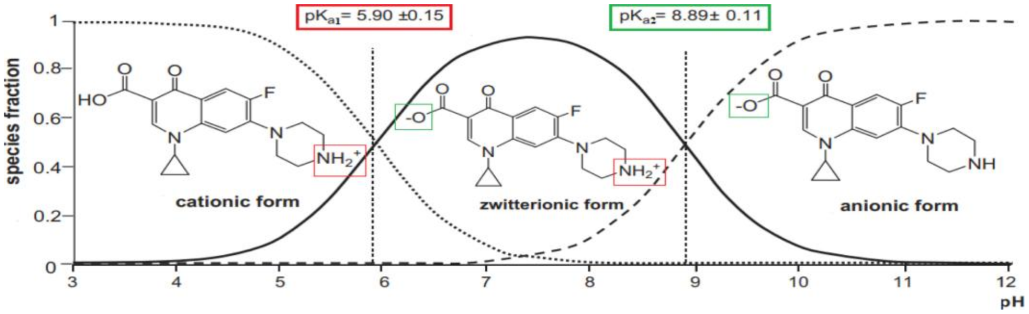

Fig. 5. Molecular structure of CIP and its ionic forms as a function of pH, pK_a values (Carabineiro, et al., 2012)

Adsorption Isotherm of MFC

The isothermic determination of the amount of CIP adsorbed on the surface of an adsorbent can be described by adsorption isotherms. In general, the number of vacant active sites and the pore size on the surface of the adsorbent play a major role in determining the amount of CIP adsorbed. Two adsorption models were applied to the adsorption of CIP on the surface of the MFC: Langmuir and Freundlich isotherms, respectively.

The adsorption isotherm models of Langmuir (Eq. (5)) and Freundlich (Eq. (6)) can be stated as follows:

$$\frac{C_e}{q_e} = \frac{1}{q_m k_l} + \frac{C_e}{q_m} \qquad (5)$$

$$\log q_e = \log k_f + \frac{1}{n}\log C_e \qquad (6)$$

The Langmuir and Freundlich models are capable of describing the adsorption mechanism on the surface and accounting for these experimental results over a greater concentration range (Juang, Wu, & Tseng, 2010). The adsorption isotherms exhibited linear curves with the highest correlation coefficients (R^2) of 0.97−0.99. The studied parameters, corresponding regression coefficients and constants for each model are listed in Table 2. After a caution resemblance between the model parameters for MFC, Langmuir was shown to be the best fitting model compared to Freundlich with $R^2 > 0.98$. Furthermore, the calculated maximum sorption capacity (q_{max}) of the Langmuir model and the experimental data values were found in good agreement with the calculated (from the model) values, confirming the validity of this model to describe the CIP sorption process. The Langmuir isotherm also suggested that sorption occurs at distinct homogeneous sites within the adsorbent surface, which is limited to monolayer sorption formation due to strong synergy between the adsorbent and the adsorbate (Rusmin, Sarkar, Liu, McClure, & Naidu, 2015). In the Figure 6 are given the adsorption isotherms of CPI adsorbed by MFC.

Table 2. Langmuir and Freundlich isotherm model parameters for CIP sorption onto MFC

Adsorbent	**Langmuir Isotherm**			**Freundlich Isotherm**		
	q_m (mg/g)	K_L x 10^{-3} (L/g)	R^2	n	K_F (L/g)	R^2
MFC	57.61	18	0.9845	1.58	2.29	0.9753

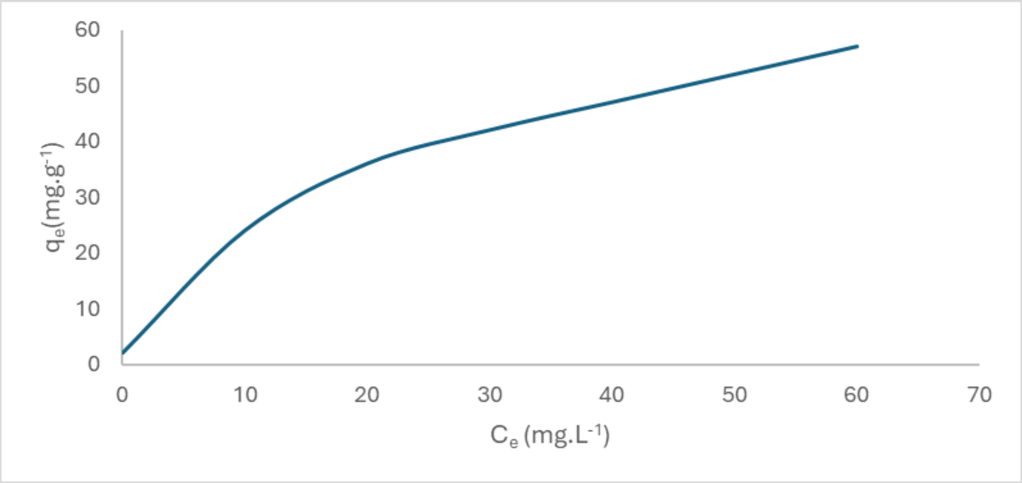

Fig. 6. Sorption isotherms modelling of CIP by Moringa-clay composite

Kinetic Adsorption Isotherm of MFC

In various fields, the pseudo-first order (PFO) and pseudo-second order (PSO kinetic models have been widely used to describe the removal of pollutants from solution (Qiu, et al., 2009). The kinetic adsorption data were adequately suited to the PFO and PSO model (Table 3). The similarity of the two models' kinetic data demonstrated that the CIP sorption process can be adequately described by the PSO model. Strong evidence for this conclusion came from the high R^2 value and good agreement between the experimental($q_{e.exp}$) and calculated sorption capacities($q_{e.cal}$) for MFC that was acquired from PSO (Table 3). As these results demonstrated, the sorption capacity of CIP on MFC via chemical sorption is dependent on the sorption rate and is based on the number of active binding sites on the adsorbents (Duan, Wang, Xiao, Zhao, & Zheng, 2018; Wu, et al., 2019).

Table 3. Pseudo-first order kinetic model and pseudo-second order kinetic model parameters.

Adsorbent	**Pseudo-first-order**				**Pseudo-second-order**			
	k_1	$q_{e.cal}$	$q_{e.exp}$	R^2	k_2	$q_{e.cal}$	$q_{e.exp}$	R^2
MFC	0.15	82.70	85.56	0.982	0.0029	87.81	85.56	0.998

The results obtained in Figure 7 showed that the sorption capacity increased rapidly in the first 40 minutes (due to fast sorption), reaching about 85% of the total CIP sorbed by MFC. After 40 minutes the rate of sorption was relatively slow and equilibrium was reached within 120 minutes for MFC.

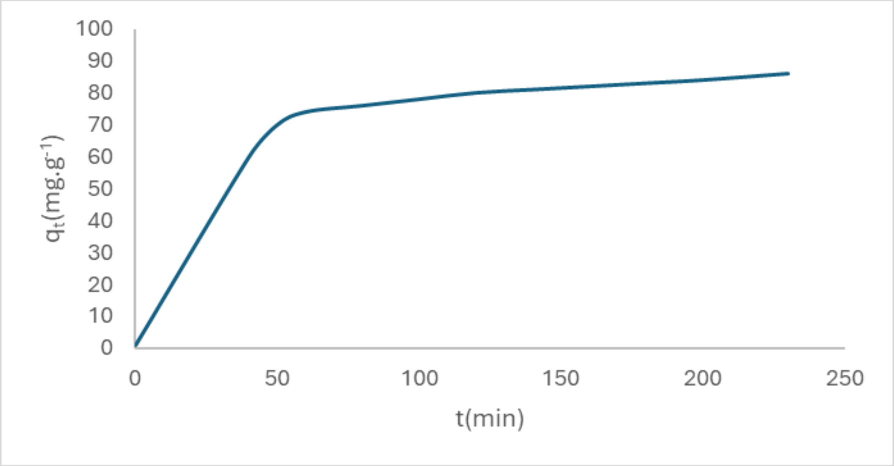

Fig. 7. Modelling of Sorption kinetics for CIP on MFC

Thermodynamics parameters determination

Numerous results can be extracted from the thermodynamic parameters, such as how strongly the adsorbate sticks to the surface of the adsorbent (i.e. chemisorption or physisorption process), exothermic or endothermic processes and entropy changes that occur throughout the adsorption process. The adsorption process is called physisorption when the ΔG° value is around 20 KJ/mol and chemisorption when the value is 80−400 KJ/mol (Wu, et al., 2013). From Table 4, CIP adsorption onto MFC is thermodynamically favourable and spontaneous as seen in the decrease of ΔG° value (Balarak, Mostafapour, & Azarpira, 2015). This is because thermal decomposition promotes the removal of water and other volatile components from the matrices of biomasses (Rocha, Pereira, Sousa, Otero, Esteves, & Calisto, 2020) and subsequent activation results in the formation of temperature-dependent active sites. The enthalpy values suggest CIP adsorption by the biosorbents is a physical process without any chemical change, thus endothermic. This physisorption, as seen in lower ΔH° values (<40 kJ/mol) obtained, is brought about by the covalent bonding between CIP molecules and biosorbent surfaces (Peñafiel, Vanegas, Bermejo, Matesanz, & Ormad, 2019). Finally, the positive ΔS° values imply that there is a rise in the degree of disorderliness and randomness during adsorption. This implies that CIP adsorption leads to disruption of hydration shell surrounding the surface of adsorbents and re-orientation of water molecules around the adsorbents surface will be less ordered.

Table 4. The determined values of thermodynamic parameters

T (K)	b (L/g)	ΔG^0 (kJ/mol)	ΔH^0 (kJ/mol)	ΔS^0 (J/molK)
288	0.19	-29	17	163

In order to assess the efficiency and feasibility of *moringa*–clay composite (MFC) in CIP removal from aqueous solution, it may be appropriate to compare its maximum adsorption capacity value with those reported in previous studies for other adsorbents. A comparison between MFC and other adsorbents with regard to their CIP adsorption capacities is presented in Table 5. According to Table 5, the adsorbents used for the adsorption of ciprofloxacin originated from different natural and synthetic materials.

Moringa-clay composite based on this comparison, has much higher adsorption capacity for CIP than the most of the studied adsorbents, and it can be a good choice as an efficient, low cost and eco-friendly adsorbent.

Table 5. CIP maximum adsorption capacities in comparison with different adsorbents

Adsorbent	Maximum adsorption capacity (mg/g)	Reference
Hazelnut based activated carbon	65	(Balarak, Mostafapour, & Azarpira, 2016)
Bamboo charcoal	36	(Wang, Chen, Ling, & Zhang, 2017)
Raw oat hulls	16	(Movasaghi, Yan, & Niu, 2019)
Synthesized Nanoceria	49.38	(Rahdar, Rahdar, Ahmadi, & Fu, 2019)
Biochar (rice straw)	131.58	(Zeng, et al., 2018)
Silica-pillared clays (Si-PILC 25)	74.5	(Roca-Jalil, Toschi, Baschini, & Sapag, 2018)
Wheat bran	159	(Khokhar, et al., 2019)
Carbon nanosheets supported TiO_2	40.5	(Li, et al., 2019)
Moringa pods-feldspar clay composite	57.61	Current study

CONCLUSION

A potential technique for enhanced removal of aqueous contaminants from solutions is a synergistic combination of inexpensive adsorbents. Well-developed pores from scanning electron microscopy and the observed functional groups from Fourier transform infrared spectroscopy demonstrated the suitability of the adsorbent to remove ciprofloxacin from aqueous solution. The optimal adsorbent dose was determined to be 0.3 g. L^{-1} and the optimal solution pH to be 7. Adsorption was observed to decrease significantly at pH values below 5, the Langmuir isotherm model best describes the adsorption data indicating that the adsorption sites were unevenly and non-specifically. Experimental data were best explained by the pseudo-second-order kinetic model. Thermodynamic studies revealed that the free energy change was negative while the enthalpy and entropy values were positive, indicating that the sorption process is endothermic and spontaneous. This study demonstrates that *Moringa oleifera* pod-modified feldspar clay composite can efficiently remove ciprofloxacin from aqueous solutions.

ACKNOWLEDGEMENTS

The authors thank the Department of Biotechnology and Chemistry, and Research Directorate, Vaal University of Technology, Vanderbijlpark, South Africa for funding this work and the support.

CONFLICT OF INTEREST

The authors declare that there is no conflict of interests regarding the publication of this article.

LITERATURE

Balarak, D., Mostafapour, F.K., & Azarpira, H. (2015). The use of low-cost adsorbent (Canola residues) for the adsorption of methylene blue from aqueous solution: isotherm, kinetic and thermodynamic studies. *J Pharm Res Int*, *7*, 16-19.

Balarak, D., Mostafapour, F.K., & Azarpira, H. (2016). adsorption kinetics and equilibrium of ciprofloxacin from aqueous solutions using *Corylus avellana* (Hazelnut) activated carbon. *Br J Pharm Res*, *13*(3), 1-14.

Carabineiro, S.A.S., Thavorn-Amornsri, T., Pereira, M.F.R., Serp, P., & Figueiredo, J.L. (2012). Comparison between activated carbon, carbon xerogeland carbon nanotubes for the adsorption of the antibiotic ciprofloxacin. *Catal Today*, *186*, 29-34.

Celik, M.S., & Ozdemir, O. (2018). Heterocoagulation of hydrophobized particulates by ionic surfactants, *Physicochem. Probl Miner Process*, *54*(1), 124-130.

Chang, X., Meyer, M.T., Liu, X., Zhao, Q., Chen, H., Chen, J., Qiu, Z., Yang, L., Cao, J., & Shu, W. (2010). Determination of antibiotics in sewage from hospitals, nursery and slaughterhouse, wastewater treatment plant and source water in Chongqing region of three Gorge Reservoir in China. *Environ Pollut*, *158*, 1444–1450.

Chen, H., Gao, B., & Li. H. (2015). Removal of sulfamethoxazole and ciprofloxacin from aqueous solutions by graphene oxide. *J Hazard Mater*, *282*, 201-207.

Cox, C.E., Marbury, T.C., Pittman, W.G., Brown, G.L., Auerbach, S.M., Fox, B.C., & Yang, J.Y. (2002). Double-blind, multicenter comparison of gatifloxacin versus ciprofloxacin in the treatment of complicated urinary tract infection and pyelonephritis. *Clin Ther*, *24*, 223–236.

Diagboya, P.N., Olu-Owolabi, B.I., & Adebowale, K.O. (2015). Effects of aging, soil organic matter, and iron oxides on the relative retention of lead, cadmium, and copper on soils. *Environ Sci Pollut Res*, *22*, 10331-10339.

Diwan, V., Tamhankar, A.J., Khandal, R.K., Shanta, S., Aggarwal, M., Marothi, Y., Iyer, R.V., Sundblad-Tonderski K., & Stålsby-Lundborg, C. (2010). Antibiotics and antibiotic-resistant bacteria in waters associated with a hospital in Ujjain, India. *BMC Public Health*, *10*, 414–422.

Dorival-García, N., Zafra-Gómez, A., Navalón, A., González, J., & Vílchez, J.L. (2013). Removal of quinolone antibiotics from wastewaters by sorption and biological degradation in laboratory-scale membrane bioreactors. *Sci Total Environ*, *442*, 317-328.

Duan, W., Wang, N., Xiao, W., Zhao, Y., & Zheng, Y. (2018). Ciprofloxacin adsorption onto different micro-structured tourmaline, halloysite and biotite. *J Mol Liq*, *269*, 874–881.

Genc, N., Dogan, E.C., & Yurtsever, M. (2013). Bentonite for ciprofloxacin removal from aqueous solution. *Water Sci Technol*, *68*, 848-855.

Gu, C., & Karthikeyan, K.G. (2005). Sorption of the antimicrobial ciprofloxacin to aluminium and iron hydrous oxides. *Environ Sci Technol*, *39*(23), 9166-9173.

Hartmann, A. (1998). Identification of fluoroquinolone antibiotics as the main source of umuC genotoxicity in native hospital wastewater. *Environ Toxico Chem*, *17*, 383–393.

Hartmann, A., Alder, A.C., Koller, T., & Widmer, R.M. (1998). Identification of fluoroquinolone antibiotics as the main source of umuC genotoxicity in native hospital wastewater. *Environ Toxicol Chem*, *17*, 377–382.

Hartmann, A., Golet, E., Gartiser, S., Alder, A.C., & Koller, T. (1999). Primary DNA damage but not mutagenicity correlates with ciprofloxacin concentrations in German hospital wastewaters. *Arch. Environ. Con. Tox*, *36*, 115–119.

Hirsch, R., Ternes, T., Haberer, K., & Kratz, K.L. (1999). Occurrence of antibiotics in the aquatic environment. *Sci Total Environ*, *225*, 109–118.

Jiang, W.T., Chang, P.H., Wang, Y.S., Tsai, Y., Jean, J.S., Li, Z., Krukowski, K. (2013). Removal of ciprofloxacin from water by birnessite. *J Hazard Mater*, *250–251*, 362-369.

Juang, R.S., Wu, F.C., & Tseng, R.L. (2010). The Ability of Activated Clay for the Adsorption of Dyes from Aqueous Solutions. *Environ Technol*, *18*, 525-531.

Khokhar, T.S., Memon, F.N., Memon, A.A., Durmaz, F., Memon, S., Panhwar, Q.K., & Muneer, S. (2019). Removal of ciprofloxacin from aqueous solution using wheat bran as adsorbent. *Sep Sci Technol*, *54*, 1278-1288.

Kümmerer, K., Al-Ahmad, A., & Mersch-Sundermann, V. (2000).

Biodegradability of some antibiotics, elimination of the genotoxicity and affection of wastewater bacteria in a simple test. *Chemosphere*, *40*, 701–710.

Kümmerer. K. (2009). Antibiotics in the aquatic environment. A review Part I. *Chemosphere*, *75*, 417–434.

Li, Z., Schulz, L., Ackley, C., & Fenske, N. (2010). Adsorption of tetracycline on kaolinite with pH-dependent surface charges. *J Colloid Interface Sci*, *351*, 254-260.

Li, B., & Zhang, T. (2012). pH significantly affects removal of trace antibiotics in chlorination of municipal wastewater. *Water Res*, *46*, 3703-3713.

Li, L., Zheng, X., Chi, Y., Wang, Y., Sun, X., Yue, Q., Gao, B.Y., & Xu, S.P. (2019). Molecularly imprinted carbon nanosheets supported TiO_2: strong selectivity and synergic adsorption photocatalysis for antibiotics removal. *J Hazard Mater*, *383*, 121211.

Liu, Y. (2009). Is the free energy change of adsorption correctly calculated? *Chem Eng J*, *54*(7), 1981-1985.

Maged, A., Kharbish, S., Ismael, I.S., & Bhatnagar, A. (2020). Characterization of activated bentonite clay mineral and the mechanisms underlying its sorption for ciprofloxacin from aqueous solution. *Environ Sci Pollut Res*, *27*, 32980-32997.

Martins, A.F., Vasconcelos, T.G., Henriques, D.M., Frank, C.S., König, A., & Kümmerer. K. (2008). Concentration of ciprofloxacin in Brazilian hospital effluent and preliminary risk assessment: a case study. *Clean*, *36*, 264–269.

Movasaghi, Z., Yan, B., & Niu, C. (2019). Adsorption of ciprofloxacin from water by pre-treated oat hulls: Equilibrium, kinetic and thermodynamic studies. *Ind Crops Prod*, *127*, 237-250.

Nasuhoglu, D., Rodayan, A., Berk, D., & Yargeau, V. (2012). Removal of the antibiotic levofloxacin (LEVO) in water by ozonation and TiO_2 photocatalysis. *Chem Eng J*, *189-190*, 41-48.

Peñafiel, M.E., Vanegas, E., Bermejo, D., Matesanz, J.M., & Ormad, M.P. (2019). Organic residues as adsorbent for the removal of ciprofloxacin from aqueous solution. *Hyperfine Interact*, *240*(1), 1-13.

Qiu, H., Lv, L., Pan, B., Zhang, Q., Zhang, W., & Zhang, Q. (2009). Critical review in adsorption kinetic models. *J Zhejiang Univ A*, *10*, 716-724.

Rahdar, A., Rahdar, S., Ahmadi, S., & Fu, J. (2019). Adsorption of Ciprofloxacin from Aqueous Environment by Using Synthesized Nanoceria. *Ecol Chem Eng S*, *26*(2), 299-311.

Roca Jalil, M.E., Toschi, F., Baschini, M., & Sapag, K. (2018). Silica pillared montmorillonites as possible adsorbents of antibiotics from water media. *Appl Sci*, *8*, 1403.

Rocha, L.S., Pereira, D., Sousa, E., Otero, M., Esteves, V.I., & Calisto, V. (2020). Recent advances on the development and application of magnetic activated carbon and char for the removal of pharmaceutical compounds from waters: A review. *Sci Total Environ*, *718*, 137272.

Rodriguez-Narvaez, O.M., Peralta-Hernandez, J.M., Goonetilleke, A., & Bandala, E.R. (2017). Treatment technologies for emerging contaminants in water: a review. *Chem Eng J*, *323*, 361–380.

Rusmin, R., Sarkar, B., Liu, Y., McClure, S., & Naidu, R. (2015). Structural evolution of chitosan-palygorskite composites and removal of aqueous lead by composite beads. *Appl Surf Sci*, *353*, 363-375.

Stuart, B. (2004). *Infrared Spectroscopy: Fundamentals and Applications*. England: John Wiley & Sons, Inc.

Sun, S.P., Guo, H.Q., Ke, Q., Sun, J.H., Shi S.H., Zhang, M.L., & Zhou, Q. (2009). Degradation of antibiotic ciprofloxacin hydrochloride by Photo-Fenton oxidation process. *Environ Eng Sci*, *26*, 753-759.

Tavengwa, N.T., Cukrowska, E., & Chimuka, L. (2016). Application of raw and biochar *Moringa oleifera* seed powder for the removal of nitrobenzene from aqueous solutions removal of nitrobenzene from aqueous solutions. *Desalin Water Treat*, *57*, 25551-25560.

Phele, M., & Mtunzi, F. (2024.). Sequestration of ciprofloxacin from aqueous solutions by nanocomposite obtained via *Moringa Oleifera* pods and feldspar clay modification. *STED Journal, 6*(2), 25-38.

Unuabonah, E.I., Gunter, C., Weber, J., Lubahn, S., & Taubart, A. (2013). Hybrid Clay: A new highly efficient adsorbent for water treatment. *Journal of Industrial and Engineering Chemistry, 132*, 252-255.

Vasquez, M.I., Hapeshi, E., Fatta-Kassinos, D., & Kümmerer, K. (2013). Biodegradation potential of ofloxacin and its resulting transformation products during photolytic and photocatalytic treatment. *Environ Sci Pollut Res, 20*, 1302-1309.

Wang, C.J., Li, Z., Jiang, W.T., Jean, J.S., & Liu, C.C. (2010). Cation exchange interaction between antibiotic ciprofloxacin and montmorillonite. *J Hazard Mater*, *183*, 309-314.

Wang, L., Chen, G., Ling, C., & Zhang, J. (2017). Adsorption of Ciprofloxacin onto bamboo charcoal: effects of pH, salinity, cations and phosphate. *Environ Prog Sustain Energy*, *36* (4), 1108-1115.

Wu, Y., Luo, H., Wang, H., Wang, C., Zhang, J., & Zhang, Z. (2013). Adsorption of hexavalent chromium from aqueous solutions by graphene modified with cetyltrimethylammonium bromide. *J Colloid Interface Sci*, *394*, 183-191.

Wu, M., Zhao, S., Jing, R., Shao, Y., Liu, X., Lv, F., Hu, X., Zhang, Q., Meng, Z., & Liu, A. (2019). Competitive adsorption of antibiotic tetracycline and ciprofloxacin on montmorillonite. *Appl Clay Sci*, *180*,105175.

Xiao, X., Zeng, X., & Lemley, A.T. (2010). Species-dependent degradation of ciprofloxacin in a membrane anodic fenton system. *J Agric Food Chem*, *58*, 10169-10175.

Yildiz, N., Erol, M., Aktas, Z., & Alimli, A.C. (2004). Adsorption of aromatic hydrocarbons on BTEA-betonites. *Adsorpt Sci Technol*, *22*, 145-154.

Zhang, D., Pan, B., Zhang, H., Ning, P., & Xing, B.S. (2010). Contribution of different sulfamethoxazole species to their overall adsorption on functionalized carbon nanotubes. *Environ Sci Technol, 44*, 3805-3811.

Zhang, C.L., Qiao, G.L., Zhao, F., & Wang, Y. (2011). Thermodynamic and kinetic parameters of ciprofloxacin adsorption onto modified coal fly ash from aqueous solution. *J Mol Liq*, *163*, 53-56.

Zeng, Z.W., Tan, X.F., Liu, Y.G., Tian, S.R., Zeng, G.M., Jiang, L.H., Liu, S.B., Li, J., Liu, N., & Yin, Z.H. (2018). Comprehensive Adsorption Studies of Doxycycline and Ciprofloxacin Antibiotics by Biochars Prepared at Different Temperatures. *Front Chem*, *6*, 80.